PAPER

The performance of a very sensitive glucose sensor developed with copper nanostructure-supported nitrogen-doped carbon quantum dots

Aysenur Aygun,[a] Esra Ozveren,[a] Ebru Halvaci,[a] Damla Ikballi,[a] Rima Nour Elhouda Tiri,[a] Cansu Catal,[a] Muhammed Bekmezci,[ab] Alper Ozengul,[a] Idris Kaynak[c] and Fatih Sen [ID] *[a]

Fluorescent glucose sensors often utilize nanotechnology to detect glucose in a sensitive and targeted manner. Nanoscale materials increase the sensitivity and efficiency of sensors by better understanding and managing the properties and interactions of the structure to be sensed. Nitrogen-doped carbon quantum dots (N-CQD), which work with the concept of fluorescence quenching or switching on because of specific processes in the presence of glucose, are one type of nanoscale material added to these sensors. In the field of biological material identification, this state-of-the-art technology is recognized as a useful tool. In this work, copper nanostructure-supported nitrogen-doped carbon quantum dots (Cu@N-CQDs) were synthesized by the hydrothermal method. The shape and structure of the fabricated materials were characterized using fluorescence (FL) spectrophotometry, Fourier Transform Infrared spectroscopy (FT-IR), transmission electron microscopy (TEM), X-ray diffraction, and UV-visible spectrophotometry (UV-vis). The proposed sensor has a linear range of 0–140 μM and a limit of detection (LOD) of 29.85 μM, showing high sensitivity and selectivity for glucose sensing by FL. The developed sensor was successfully applied to detect glucose and demonstrated the potential of Cu@N-CQDs as promising candidates for designing sensors for glucose measurement.

Introduction

The accurate, sensitive, and focused detection of glucose has several crucial applications in the biological sciences, food chemistry, and clinical technology.[1–3] For the accurate and rapid detection of glucose, many methods have been developed. For the detection of glucose, different methods are often used, such as mass spectrometry, chemiluminescence, Raman scattering, fluorescence, and electrochemistry.[4–8] Rapid and well-regulated glucose testing is essential for managing medical care and battling serious health issues like diabetes.[9] Although some limitations still exist, fluorescence spectrometry provides a possible replacement technology for electrochemical sensors for the accurate determination of glucose. Depending on the amount of glucose present in the environment, a fluorescent glucose sensor molecule can be tuned to change or increase its basic fluorescence. To provide continuous glucose monitoring, fluorescent glucose sensors can be placed in implanted structures such as capsules, microcapsules, microbeads, nano-optodes, or capillary tubes in addition to subcutaneous or intravenous catheters with removable wires.[10] However, an important area of study that has attracted attention in recent years has been the application of micro- and nanoscale materials in the field of glucose sensing.[11,12] Due to their large surface areas, superior electrical qualities, and distinctive catalytic activities, these materials make it possible to construct sensitive glucose sensors.[12,13] Numerous micro- and nanomaterials have been considered suitable sensor materials for high-performance glucose detection in this context, including transition metals and oxides, carbon-based nanomaterials like graphene, and carbon nanotubes.[14–16] In fluorescence sensors, materials with fluorescence properties or carbon derivatives that can emit fluorescence can be used.[17,18] Among carbon derivatives, carbon dots draw attention with their interesting properties.[19] One of these carbon derivatives is carbon quantum dots (CQDs).

It is one of the carbon derivatives with diameters below 10 nm. They have outstanding optical properties. In addition, these materials exhibit minimum toxicity and excellent water dispersion properties.[20,21] The highly reactive surfaces of CQDs contain different chemical groups and functional groups, which makes CQDs stand out as suitable support materials in biosensor applications and biomedical fields.[22] At the same

[a]Sen Research Group, Biochemistry Department, Faculty of Arts and Science, Kutahya Dumlupinar University, Evliya Celebi Campus, 43100, Kutahya, Turkiye. E-mail: fatihsen1980@gmail.com

[b]Department of Materials Science & Engineering, Faculty of Engineering, Dumlupinar University, Evliya Celebi Campus, 43100, Kutahya, Turkiye

[c]Machinery and Metal Technologies, Vocational School of Technical Sciences, Usak University, 1 Eylul Campus, 64200 Usak, Turkiye

time, their easy production and affordability with one-step production modeling add them to the advanced materials groups.[23] Therefore, the preparation of heteroatom-doped CQDs is of great importance for improving the optical and electrical properties of CQDs.[21,23,24] These additions are an important step in their demonstration of superior properties. For instance, nitrogen-doped carbon quantum dots (N-CQDs) for sensitive biosensing and bioimaging were efficiently prepared by a one-pot hydrothermal carbonization process with ethylene diamine, urea, melamine, and ammonia solution as an additional surface passivator.[25] Likewise, CuO nanoleaves and nitrogen-containing CQDs (CuO/NCQDs) were prepared as composites and used as photocatalysts for the photooxidation reaction.[26] There are important studies in the literature. One study reported the use of a one-step hydrothermal method to synthesize nitrogen-doped carbon quantum dots (N-CQDs) using hexamethylenetetramine as carbon and nitrogen sources. Fluorescence can be quenched by Cu^{2+} and recovered by glutathione (GSH), making N-CQDs a first-class fluorescent probe for GSH detection. N-CQDs were highlighted as promising fluorescent pH, Cu^{2+} and glutathione sensors with biocompatibility and low cytotoxicity for environmental monitoring and bioimaging applications.[27] Similarly, a report has been published on the development of a sensitive non-steroidal anti-inflammatory drug aspirin sensor utilizing copper oxide decorated with nitrogen-doped carbon quantum dots (N-CQD). The composite prepared using the electrochemical deposition method was found to exhibit a higher current response to oxidation and a good linear range of 1–907 μM, with a detection limit of 0.002 μM and a sensitivity of 21.87 μA μM^{-1} cm^{-2}. The sensor demonstrated excellent repeatability, stability, and deposition time, rendering it suitable for real-life applications.[28]

This study focuses on the application of NPs obtained by doping CQDs with nitrogen and supporting them with Cu in fluorescence sensors. The morphological properties of the NPs obtained in this study are described in detail. At the same time, it is aimed to contribute to the sensing of glucose and further studies. Our study has revealed important results in terms of the more effective use of fluorescence sensors.

Materials & method

Instruments and materials

Sigma Aldrich (USA) supplied the ethylenediaminetetraacetic acid disodium salt dihydrate (EDTA-2Na·2H$_2$O), copper chloride dihydrate, glucose (GLU), fructose (FRU), ascorbic acid (AA), dopamine (DA) reagents. TEM measurements (Joel JEM-2100), XRD measurements (Rigaku Miniflex), and fluorescence spectrum (FL) analyses (PerkinElmer LS55) were performed to evaluate the morphology of the prepared Cu@N-CQDs and to best define the structure. Fourier transform infrared (FT-IR) spectra were captured between 400 and 5000 cm^{-1} using a PerkinElmer FT-IR spectrometer. UV-vis absorbance measurements were performed with PerkinElmer lambda 750.
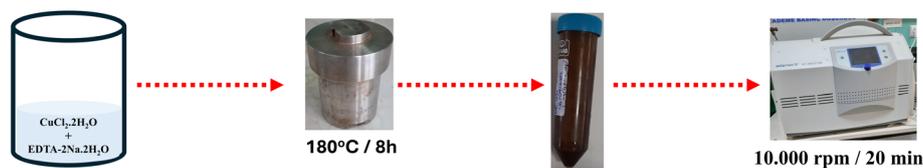
Synthesis of Cu@N-CQDs

The formation of Cu@N-CQDs was in accordance with the literature.[29] Accordingly, Cu@N-CQDs was easily synthesized by hydrothermal method using EDTA-2Na·2H$_2$O, copper chloride dihydrate (CuCl$_2$·2H$_2$O). Typically, 100 mg of EDTA-2Na·2H$_2$O and 15 mg of CuCl$_2$·2H$_2$O is dissolved in 25 ml of water. After stirring for 30 min, the resulting solution was placed in a Teflon coated autoclave. The autoclave was heated at 180 °C for 8 hours. After hydro-thermalization, the product was allowed to cool naturally to room temperature before centrifugation at 10 000 rpm for 20 min to separate the resulting solution. A 0.22 mm filtration membrane was used to purify the final product. This method: nitrogen-doped carbon quantum dots (N-CQD) are synthesized with the help of Cu^{2+} ions. During synthesis, Cu^{2+} assumes a catalytic role and is thought to help regulate the size of carbon dots. Furthermore, Cu^{2+} ions contribute to the surface exchange of carbon dots and improve surface electron transport mechanisms.[27] Copper ions in the Cu@N-CQDs structure help to optimize the fluorescence properties by successfully triggering quenching or switching on processes when the fluorescence signal interacts with glucose. As a result, the sensor is more sensitive and selective to glucose Scheme 1 shows the steps for the synthesis of Cu@N-CQDs.

Fluorescence sensing of glucose

D-Glucose solutions at concentrations between 0–140 μM were prepared in distilled water and the glucose sensing potential of the Cu@N-CQDs nanosensor was investigated. 5 μL of Cu@N-CQDs was added to 20 μL of glucose solution and incubated for 5 minutes. Then, measurements were performed in FL spectroscopy. For the selectivity test, 20 μM AA, DA, and FRU solutions were prepared and 5 μL Cu@N-CQDs was added to 20 μL solutions and incubated for 5 min. Then, measurements were performed in FL spectroscopy.

Result & discussion

After synthesis, characterization procedures were carried out for the nanostructure. In these processes, the morphological and

Scheme 1 Synthesis steps of Cu@N-CQDs.

chemical structure of the structure was discussed in detail. TEM was performed as the first analysis (Fig. 1a and b). TEM images of Cu@N-CQDs synthesized by hydrothermal methods were

obtained as in Fig. 1a and b. In the TEM picture, it can be observed that they have a roughly spherical form with a size distribution of 1 to 8 nm. It is possible that the inadequate
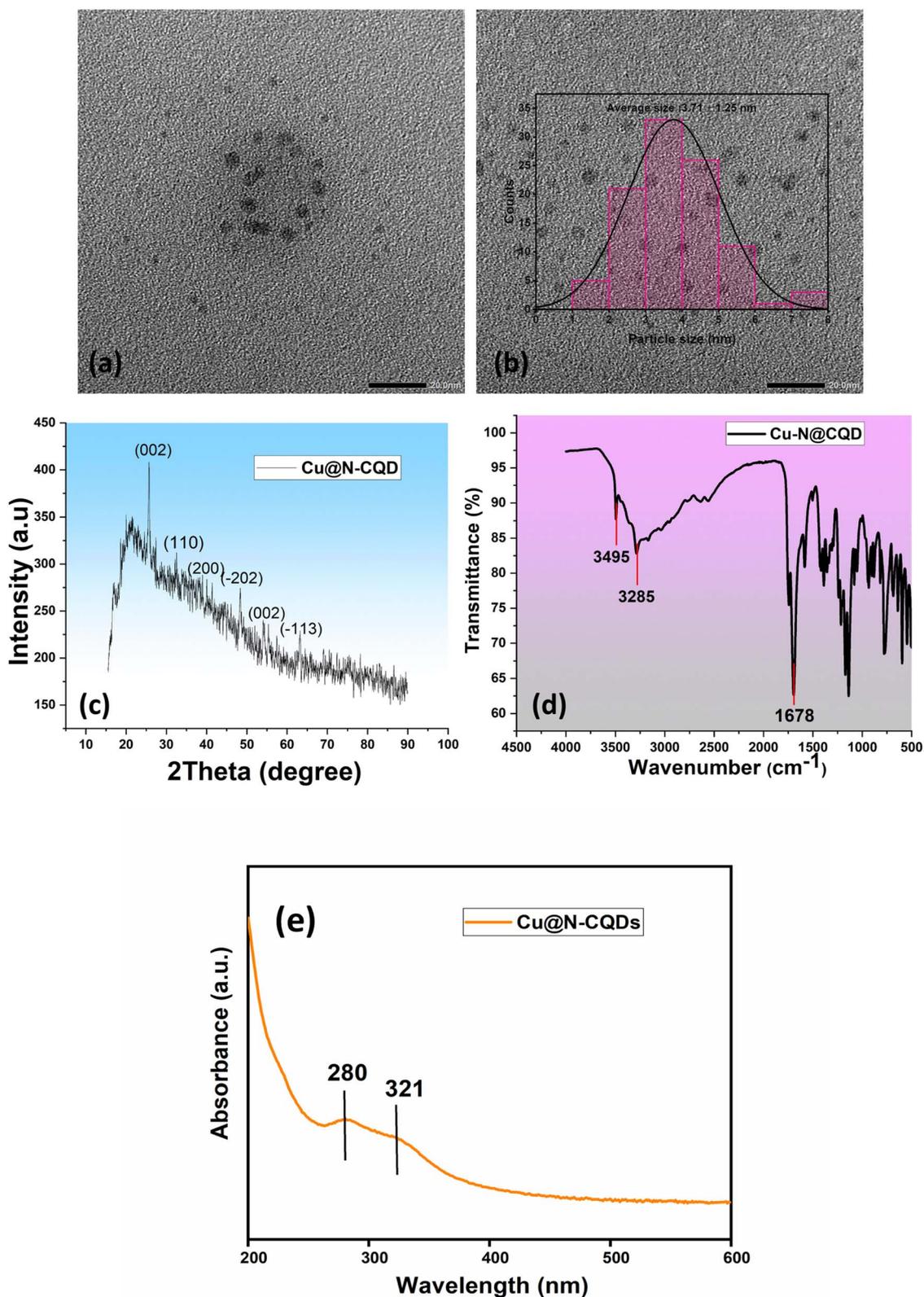

Fig. 1 (a and b) TEM images (scale, 20 nm), and particle size distribution histogram, (c) XRD patterns, (d) FTIR spectra, and (e) UV-vis spectra of Cu@N-CQDs.

separation and purification procedure is responsible for the wide size distribution. At the same time, copper-induced reduction or the presence of non-doped structures may have caused an increase in size.[30] As can be seen in the TEM image, the wide and irregular size distribution of CQDs in the 1 to 8 nm range has the potential to positively influence the detection performance. The use of CQDs of different sizes can facilitate a broader fluorescence spectrum and a spectrum with different optical properties, which collectively contributes to the formation of a more adaptable sensing system in terms of its functionality. This diversity enables the sensor to respond to changing glucose concentrations with greater versatility, and CQDs of different sizes offer both high sensitivity and a wide detection range. As a result, the overall performance of the sensor can be improved and is thus predicted to increase versatility.

Cu@N-CQDs size distribution histogram is as in Fig. 1b. According to the figure, the average diameter of the nanoparticle is approximately 3.71 ± 1.25 nm after particle counting. It can be said that this size is closely related to both copper and the size form of CQDs nanostructures.[29]

In order to have more information about the material structure, Cu–N@CQDs were also analyzed by XRD. Fig. 1c shows the XRD pattern of Cu–N@CQDs. As shown in Fig. 3, different Cu doping peaks are observed in N@CQDs. These lattice parameters can be specified as (110), (200), (−202), (002), and (−113) at the theta values of nearly 32°, 38°, 48°, 52°, and 64° respectively (CuO (JCPDS 45-0397)).[31–33] The typical carbon parameter (002) was observed at a value of about 27°. In addition, the peak at 21.5° observed in the XRD spectrum can be associated with the crystal lattice flatness of N-CQDs.[34] The results were obtained quite close to the literature.[35,36] FT-IR spectroscopy was used in the range of 4000 to 500 cm^{-1}, which was favored to identify the further surface structure and composition of Cu@N-CQDs. According to Fig. 1d, the large peak at about 3495 and 3285 cm^{-1} was attributed to the stretching vibration of O–H or N–H.[37,38] The C=O stretching vibration mode and the N–H bending mode were expressed for the main characteristic peak at 1641 cm^{-1}.[29] The peaks observed between 1000–1217 cm^{-1} correspond to the symmetrical and asymmetrical stretching vibrations of the C–O–C functional group.[39] The peaks at 1582 cm^{-1} and 1388 cm^{-1} correspond to the C=O and C–N functional groups, respectively.[38,40] The peaks observed in the 870–1000 cm^{-1} range can be attributed to N–Cu–N.[39,41] The lattice vibration modes of O–Cu can match the absorption peaks in the 500–700 cm^{-1} region.[29] Additionally, the peak at 618 cm^{-1} in the FTIR spectrum of Cu@N-CQDs corresponds to Cu–O.[42] The UV-vis spectra were illustrated in Fig. 1e, the intense peak was observed at 280 nm and a weak peak was observed at 321 nm, it may correspond to π–π* transitions of carbon double bond and n–π* transitions of carbon double bond nitrogen and carbon double bond oxygen, respectively. The obtained results are compatible with reference studies.[29,43]

The optical properties of Cu@N-CQDs were confirmed by fluorescence spectra. Fluorescence absorption (FL) spectra were shown in Fig. 2a and b. Fig. 2a illustrates the FL excitation and emission spectra, and Fig. 2b illustrates the excitation-dependent fluorescence emission spectra of Cu@N-CQDs, respectively. The fluorescence emission and excitation spectrum of Cu@N-CQDs was shown in Fig. 2a. A bright emission FL peak was observed at 415 nm with an optimum excitation wavelength of 330 nm. One of the typical features of CQDs is the "excitation wavelength dependent" emission behavior.

Fig. 2a illustrates the Cu@N-CQDs fluorescence emission and excitation spectrum. The FL measurement revealed that a noticeable emission peak with an ideal excitation wavelength of 330 nm emerged at 415 nm. One of the typical characteristics of CQDs is the emission behavior known as "excitation wavelength dependent". The strongest fluorescence was displayed by Cu@N-CQDs when the excitation wavelength was 330 nm. The fluorescence emission spectra (Fig. 2b) show a redshift about the increase in excitation wavelength from 310 to 390 nm.[39] It should be mentioned that the fluorescence emission
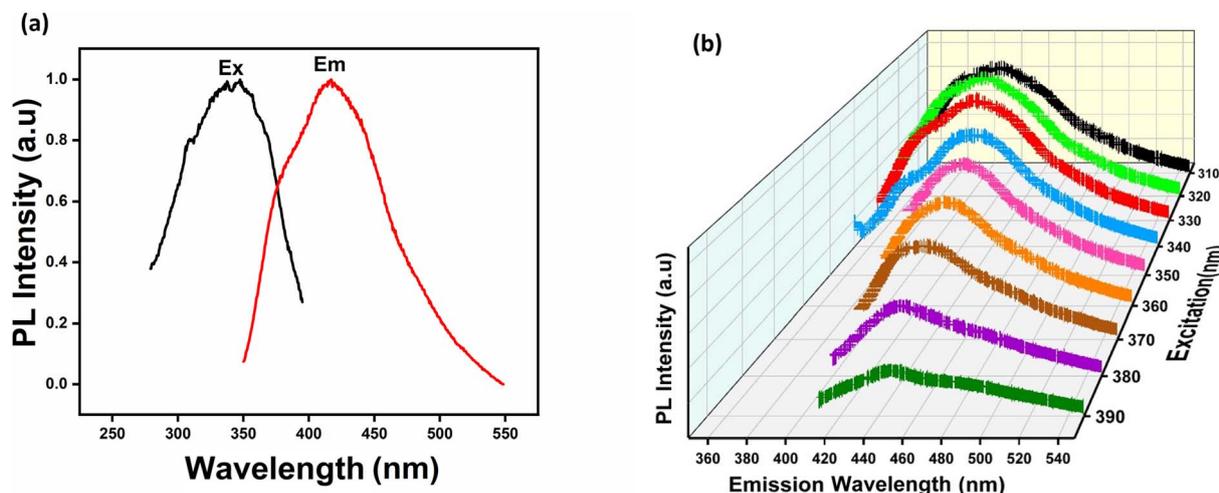

Fig. 2 (a) The emission and excitation FL spectra of Cu@N-CQDs (b) excitation-dependent fluorescence emission spectra of Cu@N-CQDs.
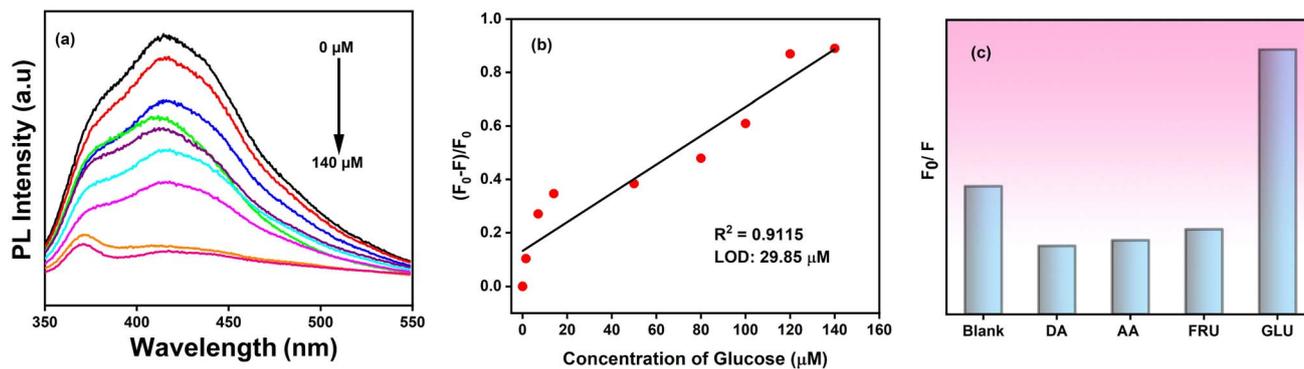
Fig. 3 (a) The emission spectra values of *versus* concentration of glucose 0–140 μM, (b) linear calibration of the fluorescence intensity ratio ((F − F_0)/F_0) and LOD value, (c) the graph of the selectivity test of the sensor towards different biomolecules (blank, DA, AA, FRU, GLU).

characteristics of the synthesized Cu@N-CQDs depend on the excitation wavelength. CQDs' optical characteristics have an enigmatic history that is still up for debate. The synthesized Cu@N-CQDs exhibit a high emission peak at 470 nm and an ideal excitation wavelength of 340 nm, according to research by Liu *et al.*[39]

After determining the emission and excitation ranges for the synthesized nanostructure, the change in wavelength in response to increasing glucose ratios was investigated. Fig. 3a shows that when the product of the glucose oxidation reaction appeared, there was a significant decrease in intensity values according to the mechanism. After examining the fluorescence properties of the synthesized material, the detection range was evaluated. The behavior of non-enzymatic sensors is almost independent of environmental conditions such as temperature, pH value, *etc.* compared to enzyme-based sensors.[44] As shown in Fig. 3a, a decrease in emission values was observed at increasing glucose ratios, indicating that it is possible to detect glucose with a label-free sensing platform. LOD was calculated for the emission peaks in response to varying concentration rates. The calculated LOD was 29.85 μM, which is a good result. Table 1 shows the comparison of the LOD value obtained with the studies in the literature. The linear curve obtained in Fig. 3b is shown. Finally, it was examined whether the nanostructure senses different biological materials. Accordingly, emission values were obtained for dopamine (DA), Ascorbic Acid (AA), and Fructose (FRU). As can be seen in Fig. 3c, the glucose ratio realized a damping close to 3 times in emission values. No damping occurred in other biological markers. This shows that the obtained sensor system is glucose selective. A glucose

fluorescence biosensor works by converting a glucose signal into an associated fluorescence signal. To correlate glucose signals with fluorescent signals in terms of peak intensity or peak decay and fluorescence lifetime, Cu@N-CQDs are good transducers. Energy transfer *via* fluorescent resonance is widely used in fluorescence-based nano-sensing systems. It is recognized as a practical and reliable analytical technique. The three main mechanisms used in fluorescent glucose nano biosensing are direct glucose binding, competitive binding, and fluorescent dye release, resulting in changes in fluorescence or fluorescence lifetime correlated with these changes.[46]

The sensor activity of Cu@N-CQDs can be explained by the fluorescence quenching mechanism (Scheme 2). The addition of glucose causes a primary change in the emission spectra of carbon dots (such as nitrogen-doped carbon quantum dots or N-CQDs) due to the interaction between the functional groups on the surface of the carbon dots and the glucose molecules. On the surface of the carbon dots, glucose molecules interact with functional groups such as hydroxyl (–OH) or amine (–NH$_2$). This interaction leads to changes in the fluorescence properties of the carbon dots, resulting in changes in the structure of the spectrum.[45] As a result of this change, the emission spectrum is altered, which can manifest as enhanced or quenched fluorescence. The surface of carbon dots can form specific interactions with glucose, which is the basis of their ability to selectively detect glucose. These groups interact electrostatically or form hydrogen bonds with the numerous hydroxyl groups present in the glucose molecule. Compared to other compounds, carbon dots exhibit a higher degree of selectivity for the detection of glucose by this method. Furthermore, under certain conditions,

Table 1 Comparison of the effect of different methods in detection of glucose

Method	System	Linear range (μM)	LOD (μM)	Reference
Colorimetry	Au–PtNCs/GO$_x$/TMB	5–55	2.4	47
Electrochemistry	GO$_x$–graphene-chitosan	80–12 000	20	48
Electrochemistry	CS–GOD–CdS–ACNTs–Pt nano	400–21 200	46.8	49
Electrochemistry (based on glucose oxidase)	SPE/sol–gel–PVA–GO$_x$	100–4550	9.8	50
Fluorometry	C-dots/AgNPs/GO$_x$	2–100	1.39	51
Fluorometry	Cu@N-CQDs	0–140	29.85	**This study**
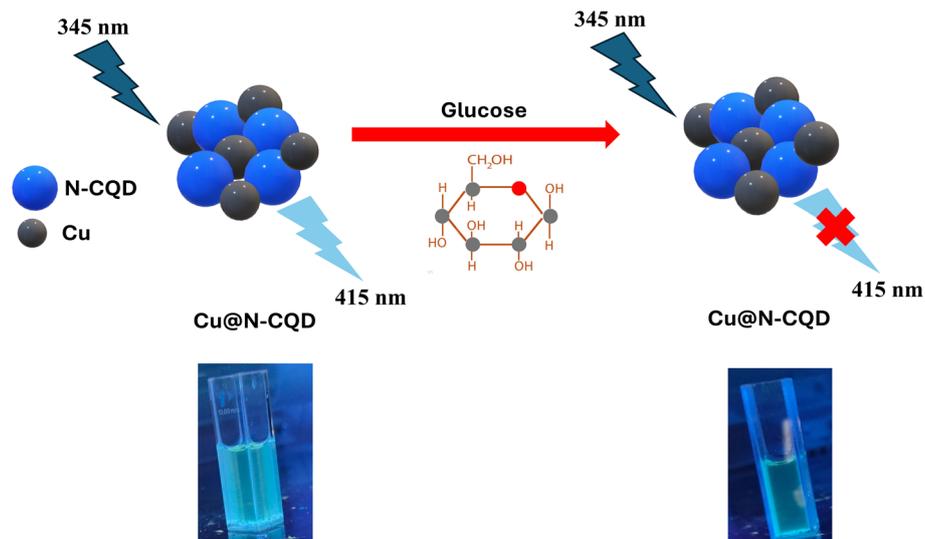
Scheme 2 The glucose detection mechanism of Cu@N-CQDs as fluorescence sensor.

synthesised Cu^{2+} ions increase the binding between glucose and carbon dots. Cu^{2+} ions bind to glucose and facilitate electron transport on carbon dot surfaces, thus increasing the selectivity of glucose detection.

Conclusion

Easy and fast detection of biomarkers is very important technological research, and especially advances in nanotechnology have led to the development of a highly selective and low-cost method for glucose detection using nanoparticles. Compared with conventional glucose sensors, fluorescence-based (FL) sensors, FL has several advantages such as simplicity in obtaining oxidation products, ease of application, and economic size. In addition, fluorescent materials obtained at low cost have also highlighted their economic dimension. As a result, Cu@N-CQDs nanostructure was synthesized in this study. The resulting structure was subjected to a series of morphological and chemical analyzes. In the histogram obtained according to the TEM analysis result, a particle of 3.71 nm in accordance with the literature was obtained. In addition, the fluorescence properties of the material were also investigated. It has been observed that the particle has emission values in the range of 400–450 nm. As a result of glucose added in the range of 0–140 μM, the quenching mechanism was activated, and the emission peak values were significantly decreased. According to these peak values, LOD was calculated as 29.85 μM. This system, which provides ease of application compared to existing methods, aims to offer a different perspective on fluorescent sensors. The results will make significant contributions to the development of CQD-based sensor systems for glucose detection.

Data availability

The data will be available upon request. Contact: aysenur.4334@gmail.com; fatihsen1980@gmail.com.

Conflicts of interest

There are no conflicts to declare.

References

1 A. Haleem, M. Javaid, R. P. Singh, R. Suman and S. Rab, *Sens. Int.*, 2021, **2**, 100100.
2 Y. Hui, Z. Huang, M. E. E. Alahi, A. Nag, S. Feng and S. C. Mukhopadhyay, *Biosensors*, 2022, **12**, 551.
3 M. Pan, X. Xie, K. Liu, J. Yang, L. Hong and S. Wang, *Nanomaterials*, 2020, **10**, 930.
4 X. Li, C. Li, S. Zhang, C. Cui, J. Li and Q. Gao, *Anal. Bioanal. Chem.*, 2021, **413**, 5725–5731.
5 Y. Li, X. Li, H. Tan and Z. Z. Huang, *Microchem. J.*, 2020, **158**, 105266.
6 E. H. Yoo and S. Y. Lee, *Sensors*, 2010, **10**, 4558.
7 F. Wang, S. Cao, R. Yan, Z. Wang, D. Wang and H. Yang, *Sensors*, 2017, **17**, 2689.
8 K. Arikan, H. Burhan, R. Bayat and F. Sen, *Chemosphere*, 2022, **291**, 132720.
9 D. M. Nathan, J. B. Buse, M. B. Davidson, E. Ferrannini, R. R. Holman, R. Sherwin and B. Zinman, *Diabetes Care*, 2009, **32**, 193–203.
10 D. C. Klonoff, *J. Diabetes Sci. Technol.*, 2012, **6**, 1242–1250.
11 B. Arman Kuzubasoglu, *ACS Appl. Electron. Mater.*, 2022, **4**, 4797–4807.
12 E. Sehit and Z. Altintas, *Biosens. Bioelectron.*, 2020, **159**, 112165.
13 S. Zhang, W. Zhao, J. Zeng, Z. He, X. Wang, Z. Zhu, R. Hu, C. Liu and Q. Wang, *Mater. Today Bio*, 2023, **20**, 100638.
14 R. Kour, S. Arya, S.-J. Young, V. Gupta, P. Bandhoria and A. Khosla, *J. Electrochem. Soc.*, 2020, **167**, 037555.
15 J. Wang, *Chem. Rev.*, 2008, **108**, 814–825.
16 Z. Zhu, L. Garcia-Gancedo, A. J. Flewitt, H. Xie, F. Moussy and W. I. Milne, *Sensors*, 2012, **12**, 5996–6022.

17 Y. Wang, J. Chen, C. Di, Y. Hu, J. C. Munyemana, Y. Shu, J.-H. Wang and H. Qiu, *Dyes Pigm.*, 2023, **212**, 111129.

18 A. P. Demchenko and M. O. Dekaliuk, *Methods Appl. Fluoresc.*, 2013, **1**, 042001.

19 J. Liu, R. Li and B. Yang, *ACS Cent. Sci.*, 2020, **6**, 2179–2195.

20 R. Atchudan, T. N. Jebakumar Immanuel Edison, M. Shanmugam, S. Perumal, T. Somanathan and Y. R. Lee, *Phys. E*, 2021, **126**, 114417.

21 P. K. Yadav, S. Chandra, V. Kumar, D. Kumar and S. H. Hasan, *Catalysts*, 2023, **13**, 422.

22 M. Farshbaf, S. Davaran, F. Rahimi, N. Annabi, R. Salehi and A. Akbarzadeh, *Artif. Cells, Nanomed., Biotechnol.*, 2018, **46**, 1331–1348.

23 S. Manzoor, A. H. Dar, K. K. Dash, V. K. Pandey, S. Srivastava, I. Bashir and S. A. Khan, *Appl. Food Res.*, 2023, **3**, 100263.

24 X. Kou, S. Jiang, S.-J. Park and L.-Y. Meng, *Dalton Trans.*, 2020, **49**, 6915–6938.

25 W. Liu, H. Jia, J. Zhang, J. Tang, J. Wang and D. Fang, *Microchem. J.*, 2020, **158**, 105187.

26 G. S. Jamila, S. Sajjad, S. A. K. Leghari and T. Mahmood, *J. Phys. Chem. Solids*, 2020, **138**, 109233.

27 S. Liao, X. Huang, H. Yang and X. Chen, *Anal. Bioanal. Chem.*, 2018, **410**, 7701–7710.

28 G. Muthusankar, R. Sasikumar, S.-M. Chen, G. Gopu, N. Sengottuvelan and S.-P. Rwei, *J. Colloid Interface Sci.*, 2018, **523**, 191–200.

29 H. Wu, Y. Yan, Q. Huang, G. Liang, F. Qiu, Z. Ye and D. Liu, *New J. Chem.*, 2020, **44**, 12723–12728.

30 J. N. Solanki, R. Sengupta and Z. V. P. Murthy, *Solid State Sci.*, 2010, **12**, 1560–1566.

31 M. Asemani and N. Anarjan, *Green Process. Synth.*, 2019, **8**, 557–567.

32 N. P. S. Acharyulu, P. Madhu Kiran, P. Kollu, R. L. Kalyani and S. V. N. Pammi, *Int. J. Eng. Res. Technol.*, 2014, **4**, 639–641.

33 S. Anwaar, Q. Maqbool, N. Jabeen, M. Nazar, F. Abbas, B. Nawaz, T. Hussain and S. Z. Hussain, *Front. Plant Sci.*, 2016, 7, 217278.

34 A. R. Sadrolhosseini, M. Beygisangchin, S. Shafie, S. A. Rashid and H. Nezakati, *Mater. Res. Express*, 2021, **8**, 105003.

35 G. Muthusankar, M. Sethupathi, S. M. Chen, R. K. Devi, R. Vinoth, G. Gopu, N. Anandhan and N. Sengottuvelan, *Composites, Part B*, 2019, **174**, 106973.

36 S. Suresh, S. Karthikeyan and K. Jayamoorthy, *J. Sci.: Adv. Mater. Devices*, 2016, **1**, 343–350.

37 H. Liang, H. Liu, B. Tian, R. Ma and Y. Wang, *Microchim. Acta*, 2020, **187**, 1–9.

38 M. Najaflu, M. Shahgolzari, F. Bani and A. Y. Khosroushahi, *ACS Omega*, 2022, **7**, 34573–34582.

39 Y. Liu, P. Wu, X. Wu, C. Ma, S. Luo, M. Xu, W. Li and S. Liu, *Talanta*, 2020, **210**, 120649.

40 S. Devi, A. Kaur, S. Sarkar, S. Vohra and S. Tyagi, *Integr. Ferroelectr.*, 2018, **186**, 32–39.

41 S. Zhuo, L. Gao, P. Zhang, J. Du and C. Zhu, *New J. Chem.*, 2018, **42**, 19659–19664.

42 B. I. Salman, *J. Fluoresc.*, 2023, **33**, 1887–1896.

43 Y. Lan, W. Bao, C. Liang, G. Li, L. Zhou, J. Yang, L. Wei and Q. Su, *Chem. Pap.*, 2023, **77**, 1005–1015.

44 H. H. Mai, D. H. Tran and E. Janssens, *Microchim. Acta*, 2019, **186**, 1–10.

45 H.-L. Yang, L.-F. Bai, Z.-R. Geng, H. Chen, L.-T. Xu, Y.-C. Xie, D.-J. Wang, H.-W. Gu and X.-M. Wang, *Mater. Today Adv.*, 2023, **18**, 100376.

46 P. D. Howes, R. Chandrawati and M. M. Stevens, *Science*, 2014, **346**, DOI: **10.1126/SCIENCE.1247390**.

47 J. Feng, P. Huang and F. Y. Wu, *Analyst*, 2017, **142**, 4106–4115.

48 X. Kang, J. Wang, H. Wu, I. A. Aksay, J. Liu and Y. Lin, *Biosens. Bioelectron.*, 2009, **25**, 901–905.

49 J. Yang, R. Zhang, Y. Xu, P. He and Y. Fang, *Electrochem. Commun.*, 2008, **10**, 1889–1892.

50 S. Zuo, Y. Teng, H. Yuan and M. Lan, *Sens. Actuators, B*, 2008, **133**, 555–560.

51 J. L. Ma, B. C. Yin, X. Wu and B. C. Ye, *Anal. Chem.*, 2017, **89**, 1323–1328.